PROCEEDINGS OF SCIENCE

Photon and π^0 electroproduction in Jefferson lab Hall A (6 GeV experiments)

Malek Mazouz[*][†]
Faculté des Sciences de Monastir, 5000 Monastir, Tunisia
E-mail: mazouz@jlab.org

Generalized Parton Distribution (GPDs) are universal functions which provide a comprehensive description of hadron properties in terms of quarks and gluons. GPDs can be accessed experimentally with hard exclusive processes such as Deeply Virtual Compton Scattering (DVCS) and deeply virtual π^0 production. Two experiments were performed in the Hall A of Jefferson Lab to measure the unpolarized cross sections of these two processes off the proton and off the neutron in the valence region (x_B=0,36) at $Q^2 \approx$2 GeV^2. After a brief description of the experimental setup, the DVCS off the proton results will be discussed and interpreted as being unexpectedly sensitive to gluons. Then, the longitudinal/transverse separation of the π^0 electoproduction cross sections, showing a dominance of the transverse terms, will be presented. Finally, an estimation of the quarks up and down contributions to the π^0 electroproduction cross sections, by combining the proton and the neutron measurements, will be shown.

XVII International Conference on Hadron Spectroscopy and Structure - Hadron2017
25-29 September, 2017
University of Salamanca, Salamanca, Spain

[*]Speaker.
[†]For the Jefferson Lab Hall A Collaboration.

1. Introduction

Generalized parton distributions (GPDs) are universal functions unifying form factors (FFs) and parton distribution functions (PDFs) involved respectively in elastic scattering and deep inelastic scattering. They encode correlations between the transverse position and the longitudinal momentum of partons inside the nucleon. At the leading order, the nucleon structure is described by eight GPDs defined for each quark flavor q. The four chiral-even GPDs (H^q, E^q, $\widetilde{H}^q$ and $\widetilde{E}^q$) conserve the parton helicity whereas the four chiral-odd or transversity GPDs (H^q_T, E^q_T, $\widetilde{H}^q_T$ and $\widetilde{E}^q_T$) flip the parton helicity [1].GPDs are accessible experimentally through hard exclusive processes such as deeply virtual Compton scattering (DVCS) and deeply virtual meson production (DVMP). At sufficiently high Q^2, the DVCS and the longitudinal DVMP amplitudes can be factorized into a hard perturbative kernel and a soft part described by GPDS as illustrated in Fig. 1 [2, 3]. The goal of our two experiments (E07-007 and E08-025) performed in the Hall A of Jefferson Lab was to study the DVCS and the π^0 electroproduction processes on the proton and the neutron by measuring their differential cross sections in the valence region ($x_B = 0.36$) at $Q^2 \in \{1.5,\ 1.75,\ 2\}$ GeV^2.

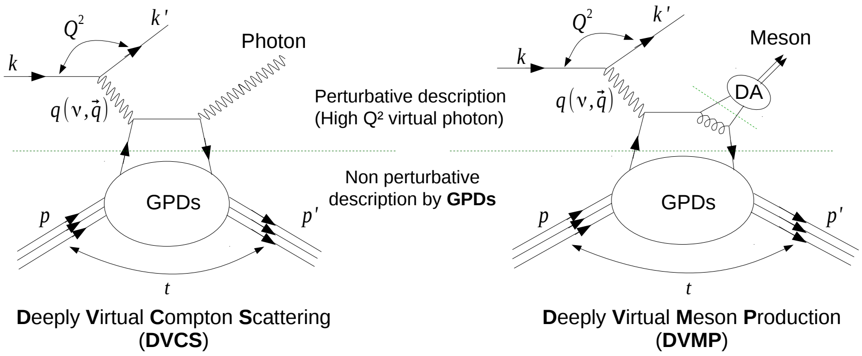

Figure 1: Leading order diagrams for DVCS and DVMP. The amplitude above the dashed factorization line can be calculated perturbatively, whereas GPDs encode the non-perturbative structure of the nucleon.

2. Experimental setup

In experiment E07-007, a few GeV electron beam was incident on a liquid H_2 (LH2) target. Two different beam energies were used for each Q^2 setting in order to perform a Rosenbluth separation of the cross section terms. We measured $\mathrm{H}(e,e'\gamma)X$ and $\mathrm{H}(e,e'\pi^0)X$ reactions by detecting the scattered electrons in a high resolution spectrometer and the emitted photons in a PbF_2 electromagnetic calorimeter. The π^0 identification in the calorimeter is based on a cut on the two-γ invariant mass. The recoil nucleon was not detected but the exclusivity of the reactions is ensured with the missing mass technique thanks to the good experimental resolution [4]. A liquid deuterium (LD2) target was used in the E08-025 experiment in order to extract the $n(e,e'\gamma)n$ and $n(e,e'\pi^0)n$ cross sections in the quasi-free approximation. The neutron contribution is deduced from a controlled subtraction of normalized Fermi-smeared LH2 data from LD2 data.

3. DVCS off the proton results

In the $\mathrm{H}(e,e'\gamma)p$ reaction, the real photon can be emitted by the proton (DVCS) or by either the incoming or scattered electron. The latter channel, called Bethe-Heitler (BH), is fully calculable with the nucleon FFs and is experimentally indistinguishable from DVCS. The $\mathrm{H}(e,e'\gamma)p$ cross section can then be written as :

$$\frac{d^4\sigma}{dx_B dQ^2 dt d\phi} = 2\,\Re e\,(T^{DVCS}\cdot T^{BH}) + |T^{BH}|^2 + |T^{DVCS}|^2 \quad . \tag{3.1}$$

Each term of the previous equation can be expressed as a sum of harmonics relatively to the angle ϕ between the leptonic and hadronic planes. The GPDs information is encoded in these harmonics through a linear combination of Compton Form factors (CFFs) in the interference term and a bilinear combination of CFFs in the DVCS^2 term. By exploiting the distinct beam energy dependences of the DVCS and BH amplitudes, we can separate the contribution of the BH-DVCS interference from the DVCS^2 contribution. Within the Braun *et al.* [5] formalism, three kind of CFFs $\mathbb{F}_{\mu\nu} \in \{\mathbb{H}_{\mu\nu}, \mathbb{E}_{\mu\nu}, \widetilde{\mathbb{H}}_{\mu\nu}, \widetilde{\mathbb{E}}_{\mu\nu}\}$, where μ and ν are the helicity state of the virtual photon and outgoing real photon, can be used to describe the DVCS process. Our accurate measurements of the $\mathrm{H}(e,e'\gamma)p$ polarized cross sections demonstrated the sensitivity of our data to twist-3 (HT) $\mathbb{F}_{0+}$ and/or next to leading order (NLO) $\mathbb{F}_{-+}$ contributions involving gluons [6]. Figure 2 shows the separation between the DVCS^2 and the BH-DVCS interference for both scenarios [6]. A significant DVCS^2 contribution to the polarized cross section difference is observed in the HT scenario, assumed to be a purely interference term in DVCS phenomenology up to now.

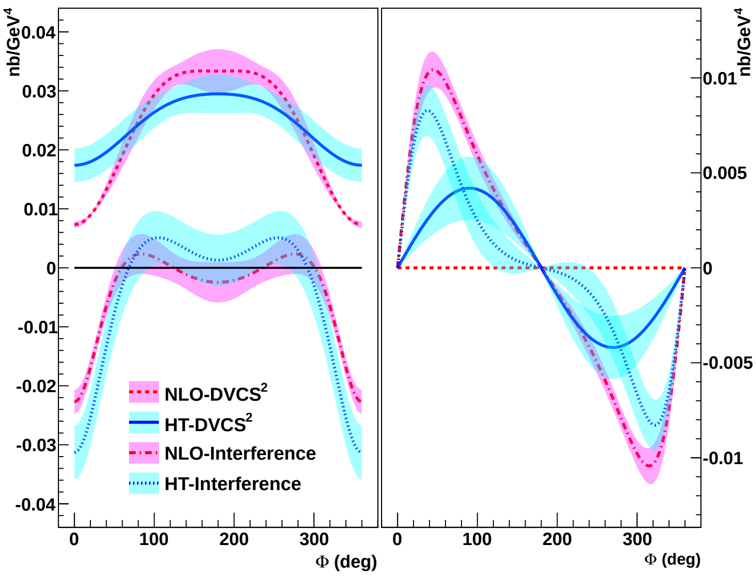

Figure 2: The DVCS^2 and DVCS-BH interference contributions at Q^2=1.75 GeV^2, x_B=0.36, t=-0.30 GeV^2 and E_{beam}=5.55 GeV for the helicity-independent (left) and helicity-dependent (right) cross sections. Solid and dotted lines represent these contributions for the HT scenario; dashed and dashed-dotted lines correspond to the NLO scenario. The bands represent the statistical uncertainty of the contributions.

4. π^0 electroproduction results

The differential cross section of deeply virtual π^0 production is given by [7]:

$$\frac{d^4\sigma}{dQ^2dx_Bdtd\phi} = \frac{1}{2\pi}\frac{d^2\Gamma_A}{dQ^2dx_B}\left[\frac{d\sigma_T}{dt}+\varepsilon\frac{d\sigma_L}{dt}\sqrt{2\varepsilon(1+\varepsilon)}\frac{d\sigma_{TL}}{dt}\cos\phi+\varepsilon\frac{d\sigma_{TT}}{dt}\cos 2\phi\right], \tag{4.1}$$

where ϕ is the angle between the hadronic and leptonic planes, $d^2\Gamma_A$ is the virtual photon flux and $\varepsilon(E_{beam})$ is the photon longitudinal polarization. The ϕ dependence of the cross section allows to extract the structure functions $\sigma_U = \sigma_T + \varepsilon\sigma_L$, σ_{TL} and σ_{TT}. The Rosenbluth separation of σ_T and σ_L is achieved for the first time thanks to cross section measurements at two different beam energies at fixed Q^2 and x_B. Figure 3 illustrates the results of this separation for the proton, the neutron and the deuteron [8, 9]. The $d(e,e'\pi^0)d$ structure functions are found compatible with zero within uncertainties. The nucleon results show a dominance of the transverse response confirming previous indications from σ_U measurements in Jefferson Lab [10, 11], while the terms involving a longitudinal response are compatible with zero within uncertainties. The interference term σ_{TT} is found negative and larger than σ_{TL}. The Bjorken regime, where a dominance of the longitudinal response is expected, is clearly not reached at our moderate Q^2 values.

Figure 3 shows also that models involving chiral-odd GPDs are in good agreement with our results within the experimental uncertainties. Actually, it was suggested in [12, 14] that a large contribution to the transverse amplitude could arise from the convolution of the transversity GPDs

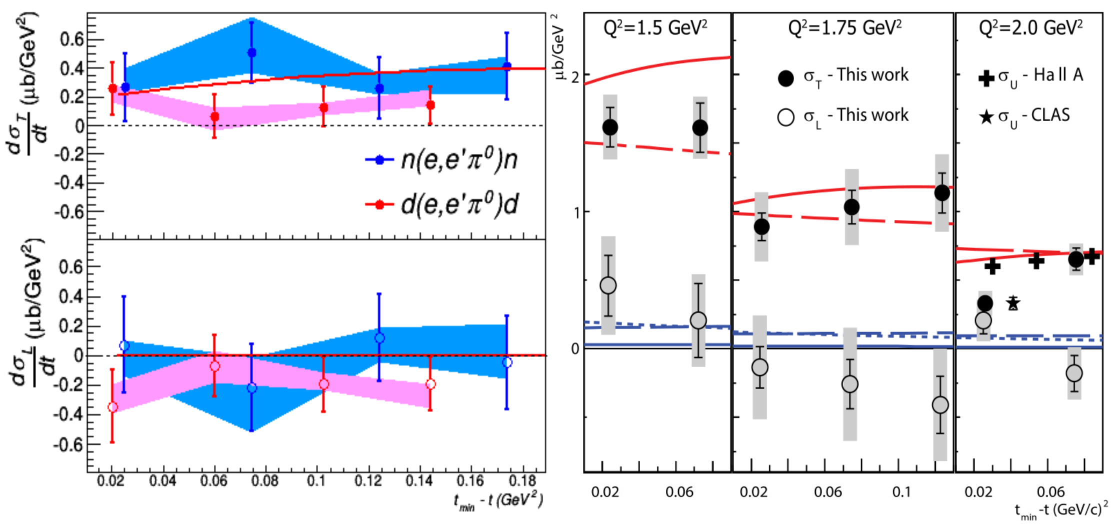

Figure 3: (Left) neutron and coherent deuteron structure functions $d\sigma_T/dt$ and $d\sigma_L/dt$ as a function of $t' = t_{min} - t$ at Q^2=1.75 GeV^2 and $x_B = 0.36$ ($x_B = 0.18$ for the deuteron). (Right) proton structure functions at Q^2=1.5, 1.75 and 2.0 GeV^2. The full lines are predictions for the nucleon from the Goloskokov-Kroll model [12] and the long-dashed lines from the Liuti-Goldstein model [13]. Bands show systematics uncertainties on the experimental data.

of the nucleon with a twist-3 quark-helicity flip pion distribution amplitude without violating the QCD factorization theorem. Within this modified factorization approach, σ_T and σ_{TT} could be written as a function of the transversity GPD convolutions $\langle H_T \rangle$ and $\langle \bar{E}_T \rangle$ ($\bar{E}_T = 2\widetilde{H}_T + E_T$) with the elementary $\gamma^* q \to q' \pi^0$ amplitude [12]:

$$\frac{d\sigma_T}{dt} = \Lambda \left[\left(1-\xi^2\right) |\langle H_T \rangle|^2 - \frac{t'}{8M^2} |\langle \bar{E}_T \rangle|^2 \right], \tag{4.2}$$

$$\frac{d\sigma_{TT}}{dt} = \Lambda \frac{t'}{8M^2} |\langle \bar{E}_T \rangle|^2 . \tag{4.3}$$

In these equations $\Lambda(Q^2, x_B)$ is a phase space factor [15] and $\xi \simeq x_B/(2-x_B)$ is the skewness variable. By combining the proton (p) and neutron (n) measurements of σ_T and σ_{TT} and by exploiting the different quark-flavor structure of the GPD convolutions for both targets :

$$\left|\left\langle H_T^{p,n} \right\rangle\right|^2 = \frac{1}{2} \left| \frac{2}{3} \left\langle H_T^{u,d} \right\rangle + \frac{1}{3} \left\langle H_T^{d,u} \right\rangle \right|^2 , \tag{4.4}$$

one can separately determine $|\langle H_T^u \rangle|$ and $\left|\left\langle H_T^d \right\rangle\right|$ (similarly $|\langle \bar{E}_T^u \rangle|$ and $\left|\left\langle \bar{E}_T^d \right\rangle\right|$) as shown in figure 4. The unknown relative phase between the u and d convolutions is treated as a systematic uncertainty in the separation. The magnitudes of the u-quark convolutions are larger than the d-quark convolutions for all t bins. These results demonstrate the possibility to access the poorly known transversity GPDs via neutral pion electroproduction in the high Q^2 regime.

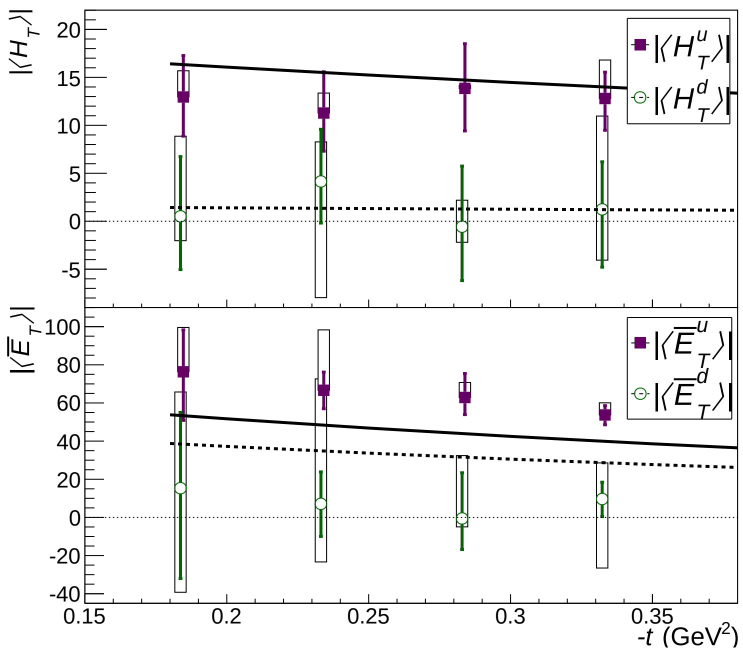

Figure 4: Magnitude of the nucleon helicity-flip $\langle H_T \rangle$ (top) and non-flip $\langle \bar{E}_T \rangle$ (bottom) transversity terms for u (squares) and d (circles) quarks assuming no relative phase between them. The boxes around the points represent the variation of the results when their relative phase varies between 0 and π. Bars show the quadratic sum of the statistical and systematic uncertainties of the data. Solid (dashed) lines are calculations from the Goloskokov-Kroll model [12] for u (d) quark.

5. Conclusion

We have quantified for the first time the individual contribution of the BH-DVCS interference term to the photon electroproduction cross section. A longitudinal/transverse separation of the π^0 electroproduction structure functions for the proton and the neutron demonstrated the dominance of the transverse response at moderate Q^2 values. Finally, new 11 GeV DVCS and π^0 electroproduction data were recently taken by our collaboration in Hall A to extend the previous measurements to a larger kinematic domain and to check the Bjorken regime validity at higher Q^2 values [16].

References

[1] M. Diehl, *Generalized parton distributions*, *Phys. Rept.* **388** (2003) 41, [hep-ph/0307382].

[2] J. C. Collins, L. Frankfurt and M. Strikman, *Factorization for hard exclusive electroproduction of mesons in QCD*, *Phys. Rev.* **D56** (1997) 2982–3006, [hep-ph/9611433].

[3] X.-D. Ji and J. Osborne, *One-loop corrections and all order factorization in deeply virtual compton scattering*, *Phys. Rev.* **D58** (1998) 094018, [hep-ph/9801260].

[4] M. Mazouz, *Energy calibration of laterally segmented electromagnetic calorimeters based on neutral pion detection*, *Nucl. Sci. Tech.* **28** (2017) 155.

[5] V. M. Braun, A. N. Manashov, D. Muller, and B. M. Pirnay, *Deeply virtual compton scattering to the twist-four accuracy: Impact of finite-t and target mass corrections*, *Phys. Rev.* **D89** (2014) 074022, [1401.7621].

[6] M. Defurne et al., *A Glimpse of Gluons through Deeply Virtual Compton Scattering on the Proton*, *Nature Comm.* **8** (2017) 1408, [1703.09442].

[7] D. Drechsel and L. Tiator, *Threshold pion photoproduction on nucleons*, *J. Phys.* **G18** 449.

[8] M. Defurne, M. Mazouz et al., *Rosenbluth separation of the* π^0 *electroproduction cross section*, *Phys. Rev. Lett.* **117** (2016) 262001, [1608.01003].

[9] M. Mazouz et al., *Rosenbluth separation of the* π^0 *electroproduction cross section off the neutron*, *Phys. Rev. Lett.* **118** (2017) 222002, [1702.00835].

[10] E. Fuchey et al., *Exclusive Neutral Pion Electroproduction in the Deeply Virtual Regime*, *Phys. Rev.* **C83** (2011) 025201, [1003.2938].

[11] I. Bedlinskiy et al., *Measurement of Exclusive* π^0 *Electroproduction Structure Functions and their Relationship to Transversity GPDs*, *Phys. Rev. Lett.* **109** (2012) 112001, [1206.6355].

[12] S. Goloskokov and P. Kroll, *Transversity in hard exclusive electroproduction of pseudoscalar mesons*, *Eur. Phys. J.* **A47** (2011) 112, [1106.4897].

[13] G. R. Goldstein, J. O. Hernandez and S. Liuti, *Flexible Parametrization of Generalized Parton Distributions from Deeply Virtual Compton Scattering Observables*, *Phys. Rev.* **D84** (2011) 034007, [1012.3776].

[14] S. Ahmad, G. R. Goldstein and S. Liuti, *Nucleon Tensor Charge from Exclusive* π^0 *Electroproduction*, *Phys. Rev.* **D79** (2009) 054014, [0805.3568].

[15] I. Bedlinskiy et al., *Exclusive* π^0 *electroproduction at* $W > 2$ *GeV with CLAS*, *Phys. Rev.* **C90** (2014) 025205, [1405.0988].

[16] J. Roche, C. Hyde, C. Muñoz Camacho et al., *Jefferson Lab Hall A experiment*, *E12-06-114* (2006) , [nucl-ex/0609015].